Dielectric Material and Foil Surface Roughness Properties Extraction Based on Single-ended Measurements and Phase Constant (β) Fitting

Shaohui Yong[#1], Victor Khilkevich[#2], Srinath Penugonda[#3], Xiao-Ding Cai[+4], Qian Gao[+5], Bidyut Sen[+6], Han Gao[+7], Douglas Yanagawa[+8], Darja Padilla[+9], Scott Hinaga[+10], James Drewniak[#11], Jun Fan[#12]
[#]EMC Laboratory, Missouri University of Science and Technology, Rolla, MO. 65401 USA
[+]Cisco Systems, Inc, San Jose, CA. 95134 USA
[1]sy2m5, [2]khilkevichv, [3]spr33, [11]drewniak, [12]jfan@mst.edu
[4]kecai, [5]annagao, [6]bisen, [7]hgao2, [8]yanagawa, [9]darja, [10]shinaga@cisco.com

***Abstract*—Dielectric substrate and foil surface roughness properties of fabricated printed circuit boards (PCB) are important for high-speed channel design. Several stripline-based extraction methods have been developed to characterize dielectric relative permittivity (ε_r), dielectric dissipation factor ($\tan\delta$), and foil surface roughness correction factor (K_R) using measured S-parameters. However, the $\tan\delta$ extraction still needs further improvement due to the difficulty in separation of dielectric and conductor loss. The authors found that the frequency-dependence of the stripline phase constant (β) is helpful to determine the $\tan\delta$ without introducing high sensitivity to foil surface roughness. By introducing a causal dielectric frequency-dependent model, ε_r and $\tan\delta$ are extracted by fitting measured β. The foil surface roughness property (correction factor K_R) is obtained using the conductor loss calculated by subtracting extracted dielectric loss from the total loss. To demonstrate the feasibility of the proposed method examples are provided using simulation data and fabricated PCB.**

***Index Terms*—Skin effect, foil surface roughness, dielectric material, striplines, printed circuit boards, signal integrity**

I. INTRODUCTION

As data rate of high-speed channels are getting higher, signal integrity (SI) performance optimization often relies on the dielectric material and foil properties. Costly re-design may occur due to the uncertainty or inaccuracy of material properties assumed during the printed circuit board (PCB) design.

The "root-omega" extraction method was developed previously to extract relative permittivity (ε_r) and dielectric dissipation factor ($\tan\delta$) by curve-fitting the measured per-unit-length (PUL) attenuation factor (α) [1-3]. However as [4-6] shown, for low-loss material with $\tan\delta$ less than 0.01, the extraction method demonstrates lack of accuracy. The extraction error goes up obviously with the increasing surface roughness level.

To overcome the drawbacks of the "root-omega" approach, a "duo-mode" extraction approach was proposed in [5] and [6]. Using the differences between the common and differential mode attenuation factors (α_{dd}, α_{cc}), $\tan\delta$ can be extracted with eliminated sensitivity to the surface roughness. Also the method does not require any *a priori* information about the frequency-dependent behavior of the dielectric properties, which might help to capture the actual frequency-dependence of $\tan\delta$. However, the "duo-mode" extraction approach requires strongly-coupled striplines to achieve large enough differences between α_{dd} and α_{cc}. Thus, weakly-coupled, single-ended or differential probe [7] measured striplines are not applicable, which limits the usage of the "duo-mode" extraction approach.

As the drawbacks of the previous approach are evident, a new single-ended measurement-based method is proposed in this paper. Compared to the "root-omega" approach, the new method can potentially reduce the extraction error by using the measured phase (β) to determine $\tan\delta$. Compared to the "duo-mode" approach, the proposed method still uses a specific approximation for the complex permittivity of the dielectric, but the restriction of strongly-coupled lines is lifted.

As a part of the paper organization, in Section II, the analysis in the frequency-dependence of the phase constant (β) is performed to reveal the mechanism of the proposed extraction method. In Section III, the extraction method is validated using simulation data. In Section IV, extraction results using fabricated PCB are shown.

II. THE EXTRACTION METHODOLOGY

A. The Lossy Transmission-lines Modeling

Before describing the extraction method, we would like to introduce the necessary parameters for the lossy transmission-line modeling. Suppose the propagation constant (γ) of a single-ended stripline is known (measured). We know that γ is related to the PUL parameters of the stripline [8]:

$$\gamma = \sqrt{(R_H + j\omega L_H)(G + j\omega C)} \quad (1)$$

where G, C, R_H and L_H represent the PUL conductance, capacitance, resistance and inductance of a stripline with rough conductor surfaces (subscript H indicates that the parameters depend on roughness). For practical low-loss transmission-lines $R_H \ll j\omega L_H$ and $G \ll j\omega C$. Using Taylor series expansion, the attenuation factor (α) and phase constant

This paper is based upon work supported partially by the National Science Foundation under Grant No. IIP-1916535.

(β) are expressed in this case as [8]:

$$\alpha = \text{real}(\gamma) \approx \frac{1}{2} R_H \sqrt{\frac{C}{L_H}} + \frac{1}{2} G \sqrt{\frac{L_H}{C}} \qquad (2)$$

$$\beta = \text{imag}(\gamma) \approx \omega \cdot \sqrt{C \cdot L_H} \qquad (3)$$

Next, let us express α and β using parameters determined by the cross-sectional geometry and the material properties by separating PUL C, G, R_H and L_H.

The capacitance (C) can be calculated by scaling the capacitance of the air-filled transmission line C_{air} (i.e. the capacitance calculated from the geometry only) by the dielectric relative permittivity (ε_r) [9, (4.36)]:

$$C = C_{air} \cdot \varepsilon_r \qquad (4)$$

The PUL conductance (G) of the line is related to the dielectric dissipation factor ($\tan\delta$) under the assumption of homogeneous dielectric material [9, (4.110)]:

$$G = \tan\delta \cdot \omega \cdot C \qquad (5)$$

Foil surface roughness causes an increment in resistance and internal inductance of the conductor. Following [10-13] the resistance correction factor (K_R) and internal inductance correction factor (K_L) can be introduced:

$$R_H = R \cdot K_R, \qquad (6)$$

$$L_H = L_{ex} + L_{in,H} = L_{ex} + L_{in} \cdot K_L, \qquad (7)$$

where the resistance, external inductance and internal inductance of the stripline with smooth conductors are expressed as R, L_{ex} and L_{in}. By inserting (4-7) into (2) and (3), the attenuation factor (α) and phase constant (β) can be calculated using the parameters depending on the geometrical dimensions only ($R, C_{air}, L_{in}, L_{ex}$) and on the PCB material properties (K_R, K_L, ε_r, $\tan\delta$):

$$\alpha = \frac{1}{2} \cdot R \cdot K_R \cdot \sqrt{\frac{C_{air}}{L_{ex} + L_{in} \cdot K_L}} \cdot \sqrt{\varepsilon_r} + \frac{1}{2} \cdot \tan\delta \cdot \omega \cdot \sqrt{C_{air} \cdot (L_{ex} + L_{in} \cdot K_L)} \cdot \sqrt{\varepsilon_r} \qquad (8)$$

$$\beta = \omega \cdot \sqrt{C_{air} \cdot \varepsilon_r \cdot (L_{ex} + L_{in} \cdot K_L)} \qquad (9)$$

To ensure causality, the dielectric material's properties $\varepsilon_r(\omega)$ and $\tan\delta(\omega)$ should satisfy the Kramers-Kronig (K-K) relations [12, Equ. (6-34)]:

$$\varepsilon_r(\omega) = 1 + \frac{2}{\pi} \int_0^\infty \frac{\omega' \varepsilon_r(\omega') \tan\delta(\omega')}{(\omega')^2 - \omega^2} d\omega'$$

$$\tan\delta(\omega) = \frac{1}{\varepsilon_r(\omega)} \cdot \left(-\frac{2\omega}{\pi} \int_0^\infty \frac{1 - \varepsilon_r(\omega')}{(\omega')^2 - \omega^2} d\omega' \right) \qquad (10)$$

Since the rough metal impedance $Z_H = R_H + j\omega L_H$ must be a causal function [11], the internal inductance correction factor (K_L) and resistance correction factor (K_R) should also meet the K-K relations to ensure causality [12, Appendix E]:

$$R(\omega) K_R(\omega) = 1 + \frac{2}{\pi} \int_0^\infty \frac{\omega' [L_{ex} + L_{in}(\omega') K_L(\omega')]}{(\omega')^2 - \omega^2} d\omega'$$

$$L_{ex} + L_{in}(\omega) K_L(\omega) = -\frac{2\omega}{\pi} \int_0^\infty \frac{1 - R(\omega') K_R(\omega')}{(\omega')^2 - \omega^2} d\omega' \qquad (11)$$

The cross-sectional geometry of the stripline under investigation might be known, and in that case R, C_{air}, L_{ex}, L_{in} can be calculated using a 2D solver. Theoretically, the remaining unknown parameters K_R, K_L, ε_r and $\tan\delta$ can be obtained by solving a system of equations (8), (9), (10) and (11). However the system cannot be solved analytically, and the integral transform in (10) and (11) converges poorly if the integral is taken on the limited frequency interval. As an alternative to solving the system of equations, the authors would like to bring up reasonable assumptions by analyzing the sensitivity of α and β to surface roughness (K_R, K_L) and dielectric dissipation factor ($\tan\delta$), so that the equations (8) or (9) might be simplified for potential solvable solutions. Also, to avoid the complicated K-K relations expressions, the causality expressions (10) and (11) can be replaced by assuming a certain causal dielectric and roughness models, such as the Djordjevic model [14] [15] and causal Huray model [10].

B. Sensitivity Analysis

To reduce the number of unknown parameters the sensitivity analysis is performed using simulation data. A 2D model of the single-ended stripline with the cross-sectional dimensions indicated in Fig.1 was created. The nodal PUL parameters (R, C_{air}, L_{in}, L_{ex}) of the model were calculated by solving a 2D cross-sectional problem using Ansys Q2D [16] and illustrated in Fig.2.

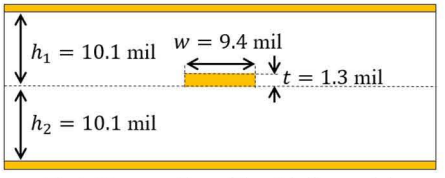

Fig.1. Cross-section of the stripline model.

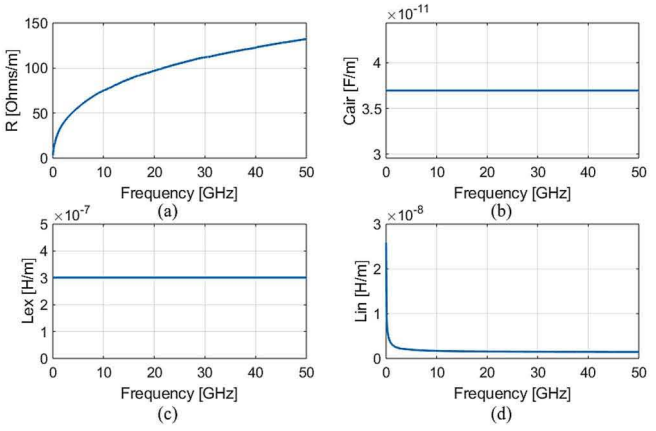

Fig.2. PUL parameters of the stripline model (a) resistance R; (b) capcitance C_{air}; (c) external inductance L_{ex} claculated for conductor conductivity set to 5.8e30 S/m (practically a PEC); (d) internal inductance L_{in} calcualted using the difference between L_{ex} and the total inductance L of the model with conductor conductivity set to 5.8e7 S/m (copper).

Several realistic examples are then created to show the impact from surface roughness on α and β. The foil surface roughness is modeled using the causal Huray model [10] with ball size $a = 0.5\mu$m and the tile area $A = 50\mu\text{m}^2$. the number of balls (N) is swept from 0 to 30 to simulate foil surfaces with RMS roughness from 0 to 2.0 μm (foil types from HVLP with

0.4μm RMS roughness, to STD with 1.8μm RMS roughness are covered). The surface roughness correction factors (K_R, K_L) are illustrated in Fig. 3 (a, b). Dielectric material's properties are the controlled variables for this experiment. Djordjevic model [14] [15] is used to model the low-loss dielectric with $\varepsilon_r = 3.4$ and $\tan\delta = 0.004$ at 1 GHz. The α and β with different surface roughness are calculated using (8, 9) and illustrated in Fig. 3 (d,e). We can observe that the attenuation factor (α) is sensitive to the surface roughness, with almost 40% increase at 50GHz for the roughest case. The foil roughness impact on β can be defined as the absolute difference of β (normalized to frequency to remove the linear part of the phase progression) for smooth and rough surfaces, which gives the following quantities for STD and HVLP foils:

$$\frac{\Delta\beta_{STD}}{\omega} = \left(\frac{\beta|_{N=30}}{\omega}\right) - \left(\frac{\beta|_{N=0}}{\omega}\right)$$
$$\frac{\Delta\beta_{HVLP}}{\omega} = \left(\frac{\beta|_{N=10}}{\omega}\right) - \left(\frac{\beta|_{N=0}}{\omega}\right) \quad (12)$$

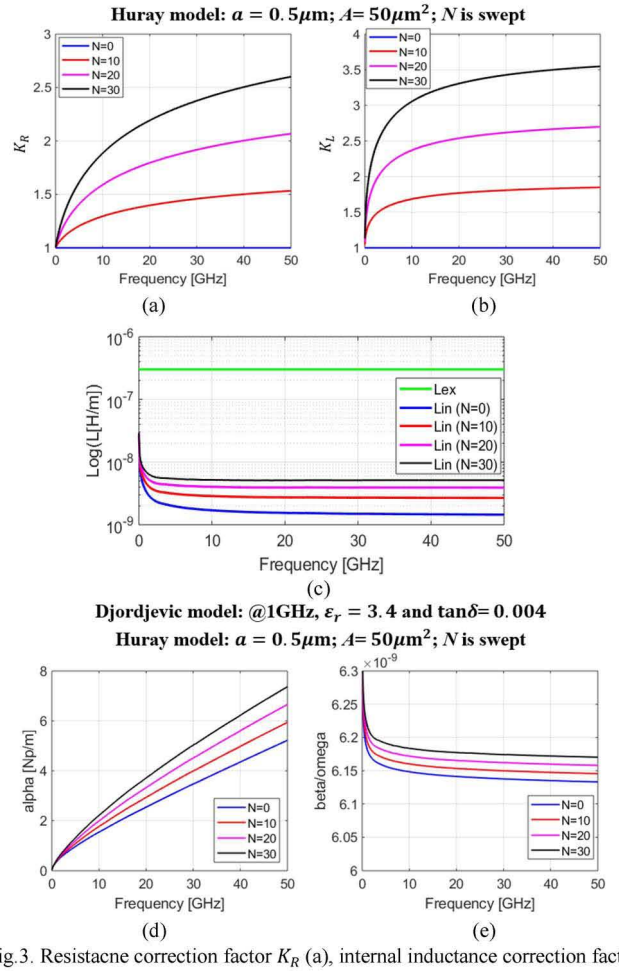

Fig.3. Resistacne correction factor K_R (a), internal inductance correction factor K_L (b) and internal inductances (c) for different roughness levels., α and β modeled using different K_R and K_L are shown in (d) and (e) for same dielectric model.

Examples are also generated to present the impact from dielectric dissipation to α and β. At 1GHz the dielectric material has $\varepsilon_r = 3.4$, and $\tan\delta$ is swept from 0 to 0.012 using Djordjevic model (low-loss to high-loss materials are covered). According to Fig. 4(a, b), it can be observed that higher $\tan\delta$ tends to cause stronger frequency-dependence in ε_r. The surface roughness correction factor is the controlled variable for this experiment with the number of balls (N) set to 10. The attenuation factors calculated using (8) and (9) are shown in Fig. 4(c, d). It is very obvious that both α and $\beta$are sensitive to the dielectric dissipation ($\tan\delta$). By assuming $\tan\delta = 0.012$ for high-loss dielectric and $\tan\delta = 0.004$ for the low-loss dielectric, it is possible to introduce corresponding differences for the phase constant relative to the lossless case:

$$\frac{\Delta\beta_{HighLoss}}{\omega} = \left(\frac{\beta|_{\tan\delta=0}}{\omega}\right) - \left(\frac{\beta|_{\tan\delta=0.012}}{\omega}\right)$$
$$\frac{\Delta\beta_{LowLoss}}{\omega} = \left(\frac{\beta|_{\tan\delta=0}}{\omega}\right) - \left(\frac{\beta|_{\tan\delta=0.004}}{\omega}\right) \quad (13)$$

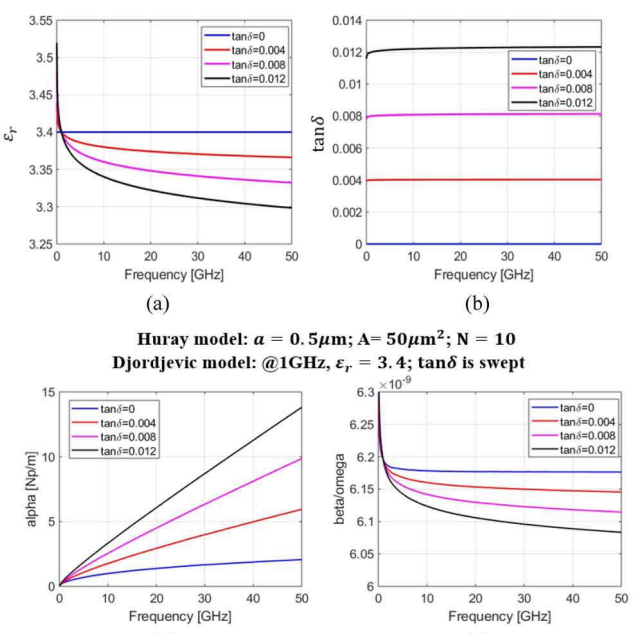

Fig.4. ε_r (a) and $\tan\delta$ (b) for different didlectric loss. In (c) and (d), α and β are calcualted using the dielectric data in (a) and (b).

Comparison between the absolute difference in phases defined by (12) and (13) is illustrated in Fig.5. The authors find that the impact from surface roughness ($\Delta\beta_{STD}/\omega$ and $\Delta\beta_{HVLP}/\omega$, the blue curves in Fig.5) is always relatively frequency-independent when compared to the influence from dielectric material ($\Delta\beta_{HighLoss}/\omega$ and $\Delta\beta_{LowLoss}/\omega$, the red curves in Fig.5). This conclusion holds even when comparing $\Delta\beta_{HighLoss}/\omega$ with $\Delta\beta_{HVLP}/\omega$, meaning that the impact from very rough surface roughness (RMS equals to 2.0 μm) is still frequency-independent when compared to the impact from ultra-low-loss dielectric material ($\tan\delta$ is about 0.004). Such phenomenon indicates that the frequency-dependence of β is mainly dependent on the dielectric dissipation factor ($\tan\delta$), but not on the conductor roughness.

Let's take a closer look at β given by expression (9). The frequency-dependence of (β/ω) is determined by ε_r and internal inductance ($K_L \cdot L_{in}$), considering that C_{air} and L_{ex} are practically frequency-independent (Fig. 2). By observing the data shown in Fig.3 (b, c), we find that:

- For frequencies below 1 GHz, the value of K_L is close to one, meaning that:

$$L_{in} \cdot K_L \approx L_{in} \quad (14).$$

- For frequencies above 1GHz, even though K_L goes up as frequency increases, the total internal inductance is very small due to reduced skin depth:

$$L_{in} \cdot K_L \ll L_{ex} \quad (15).$$

Both above conditions will be satisfied by the following approximation:

$$L_H = L_{ex} + L_{in} \cdot K_L \approx L_{ex} + L_{in} \quad (16)$$

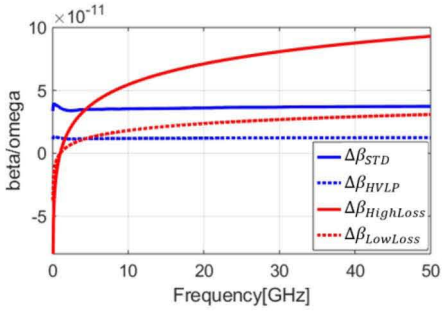

Fig.5. By calculating the absolute difference in β/ω, the influence of roughness and dielectric loss on the frequency dependency of phase is illustrated.

To summarize:

- The impact form surface roughness to the frequency-dependence of β is very limited. By inserting (16) into (9), β can be estimated by ignoring K_L:

$$\beta \approx \omega \cdot \sqrt{C_{air} \cdot \varepsilon_r \cdot (L_{ex} + L_{in})} \quad (17).$$

- The frequency-dependence of β is mainly determined by ε_r, which is related to the $\tan\delta$ due to causality.

C. The Extraction Methodology

By using (17), the initial value of relative permittivity (ε_{r0}) is determined from the measured β, and simulated PUL C_{air} and L:

$$\varepsilon_{r0} = \left(\frac{\beta}{\omega}\right)^2 \cdot \frac{1}{C_{air} \cdot (L_{in} + L_{ex})} \quad (18)$$

A user-preferred causal dielectric material model (such as Djordjevic model or 2-term Djordjevic model [6]) is selected and the model parameters are determined by curve fitting. In this paper, we use the trust region methods to perform nonlinear least-squares curve fitting [17]. The objective function (T_ε), defined as the integral (or sum in case of discretized quantities) of the squared difference between the modeled dielectric permittivity ($\varepsilon_{r,\text{model}}$) and the initially extracted permittivity (ε_{r0}) along frequencies is minimized, producing the extracted $\varepsilon_{r,\text{ext}}$:

$$T_\varepsilon = \int_{f_1}^{f_2} \left|\varepsilon_{r,\text{model}}(f) - \varepsilon_{r0}(f)\right|^2 df \quad (19)$$

$$\min(T_\varepsilon) = \int_{f_1}^{f_2} \left|\varepsilon_{r,\text{ext}}(f) - \varepsilon_{r0}(f)\right|^2 df \quad (20)$$

where the lowest and highest measured frequency points are f_1 and f_2. The optimized $\varepsilon_{r,\text{ext}}$ is the extracted dielectric permittivity, and the extracted $\tan\delta_{\text{ext}}$ is available using the K-K relations (10).

After the extraction of the dielectric material properties, the modeled dielectric attenuation factor is subtracted from the measured attenuation factor. The surface roughness correction factor is then calculated as:

$$K_{R0} = \frac{\alpha - \frac{\omega}{2} \cdot \tan\delta_{\text{ext}} \cdot \sqrt{C_{air}(L_{ex} + L_{in})\varepsilon_{r,\text{ext}}}}{\frac{R}{2} \cdot \sqrt{\frac{C_{air}}{L_{ex} + L_{in}}} \cdot \sqrt{\varepsilon_{r,\text{ext}}}} \quad (21)$$

To obtain smooth extraction results, a user-preferred surface roughness model (such as Huray model [10] or Hemispherical model [15]) is used to fit K_{R0}. After minimizing the integral of the difference between modeled resistance correction factor and K_{R0}, the extracted $K_{R,\text{ext}}$ is obtained.

III. Numerical Validations

To illustrate feasibility and accuracy of the proposed method, a 2D model of the stripline with the cross-sectional dimensions indicated in Fig. 1 was created. The dielectric material has $\varepsilon_r = 3.4$ and $\tan\delta = 0.003$ at 1GHz and is modelled according to Djordjevic. The surface roughness is modeled using the Huray model with ball size $a = 0.58\mu$m, number of balls $N = 5$ (HVLP2 foil treatment, RMS roughness is about 0.25μm), and the tile area $A = 50\mu\text{m}^2$.

The values of ε_r, $\tan\delta$ and K_R extracted using the methodology described above while assuming the Djordjevic model for the dielectric are shown in Fig. 6. For the extracted ε_r, the extracted value is slightly larger than the actual one because the initially extracted ε_r ($\varepsilon_{r,0}$) is calculated under the assumption of $K_L = 1$, but the error is small, and does not exceed 0.3 %. The extraction errors for $\tan\delta$ and K_R are both below 1.5%.

To test the sensitivity of the extracted ε_r and $\tan\delta$ to surface roughness, several cases with different surface roughness are modeled. The surface roughness is modeled using Huray model with the number of balls N swept from 0 to 30 (RMS roughness from 0 to 2.0 μm).

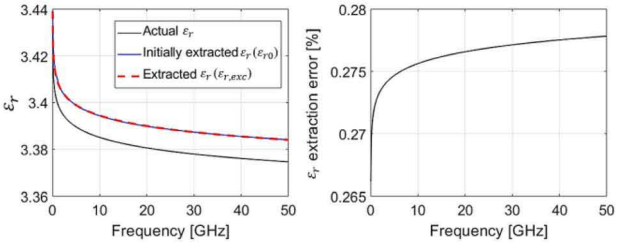

(a)

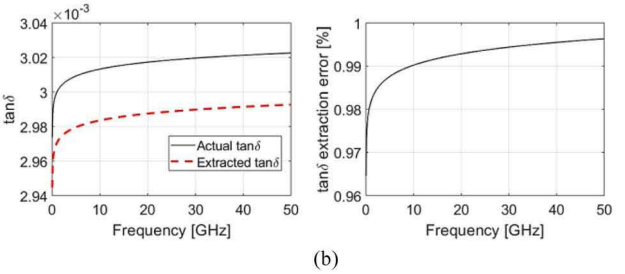

(b)

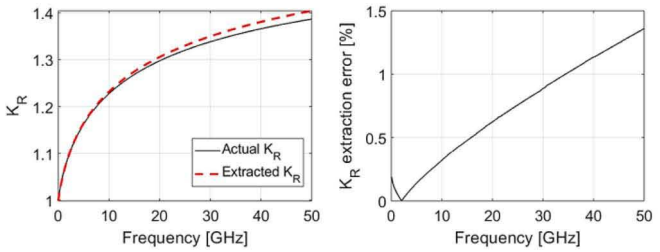

(c)

Fig.6. Comparision between the actual and extracted ε_r (a), tanδ (b) and K_R (c) for a simulated transmission line.

The extracted ε_r and tanδ are shown in Fig.7. It can be observed that the extraction error increases as rougher foil surface is introduced. Since the extraction approach assumes that surface roughness has a negligible impact on the phase constant (β), larger K_L due to rougher surface will violate the assumption of $K_L = 1$ and make the frequency-dependence of β depend more on the increasing K_L instead of ε_r. Thus, the proposed extraction approach cannot separate the dielectric and conductor attenuation perfectly. However, even in the slightly unrealistic worst with a very rough conductor (RMS roughness 2.0 μm, STD foil treatment) and ultra-low-loss dielectric material (tanδ is about 0.003), the tanδ extraction error is still below 7%. Compared to the "Root-Omega" extraction results with more than 10% error when RMS roughness is larger than 0.5 μm [5], we would like to conclude that the proposed algorithm has significant improved extraction accuracy.

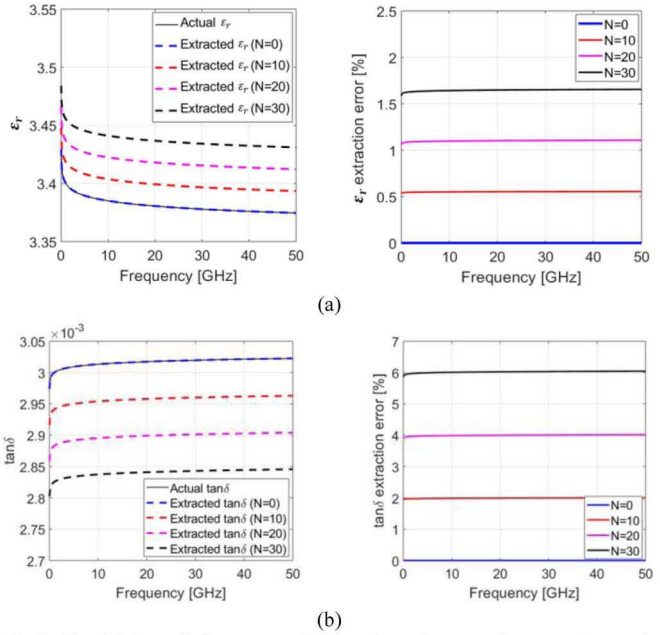

(a)

(b)

Fig.7. Sensitivity of the extracted ε_r and tanδ to surface roughness is demonstrated by sweeping RMS foil roughness from 0 to 2.0 μm

IV. Extraction Using Measured Data

To test the proposed method, a validation board containing multiple lines was fabricated. Two of the lines (1.3 inches and 15.8 inches) were used for 2x-thru measurements [18-20]. Previously, this testing vehicle's properties have already been extracted using the "duo-mode" approach [5] [6]. In this section we are going to use the measured S_{cc21} to extract material properties and compare with the results of the "duo-mode" approach.

The de-embedded common mode S-parameters is given in Fig.8. Using the known cross-sectional geometry, the common mode PUL parameters (R_{cc} , $C_{air,cc}$, $L_{ex,cc}$, $L_{in,cc}$) are calculated by Ansys Q2D. The extraction results using Djordjevic dielectric model is shown in Fig. 9. We can observe that the Huray modeled surface roughness correction factor does not have a good match with the initially extracted K_{R0} calculated using (20). The modeled attenuation factor using extracted ε_r , tanδ and K_R overestimates the loss for frequencies below 20GHz and underestimate the loss for frequencies above 20GHz.

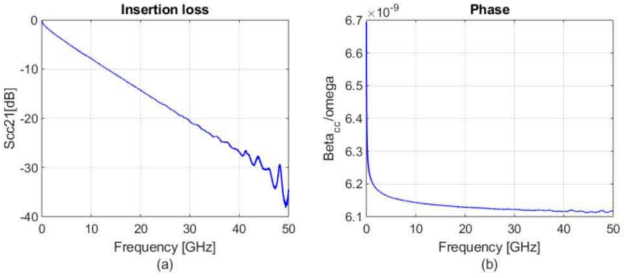

Fig. 8. De-embedded common mode insertion loss (a) and phase (b) for the 15.8-inch line using the 1.3-inch line as a thru.

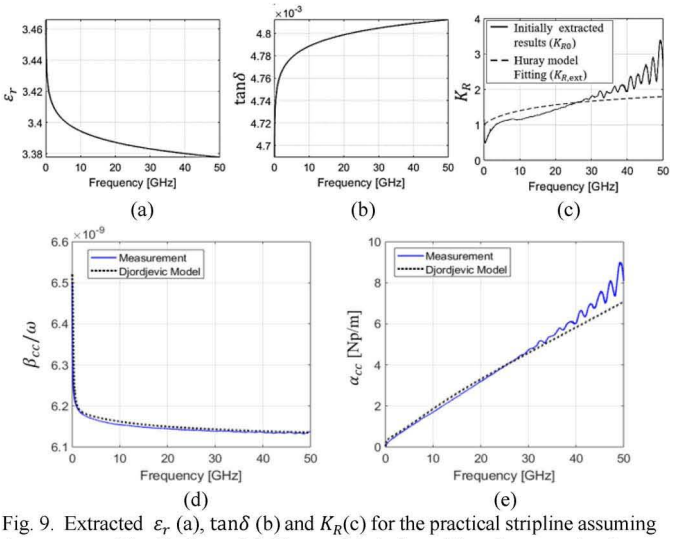

Fig. 9. Extracted ε_r (a), tanδ (b) and K_R(c) for the practical stripline assuming the one-term Djordjevic model. The modeled phase (d) and attenuation factor (e) are compared with the measurement results.

As can be seen from Fig. 9 (b), the Djordjevic model outputs practically frequency-independent tanδ, and does not allow to model the strongly frequency-dependent dielectric loss as reported in [6]. To improve the extraction results, the extraction process is repeated for the two-term Djordjevic model [6]. The first-term of the model is characterized by independent parameters $\Delta\varepsilon_1$, $\varepsilon_{\infty 1}$ and fixed lower and higher frequencies equal to $f_{1,1}$ =1kHz and $f_{1,2}$ =10THz; the second-term has independent parameters $\Delta\varepsilon_2$, $\varepsilon_{\infty 2}$ and fixed lower and higher frequencies equal to $f_{2,1}$ =30GHz and $f_{2,2}$ =10THz. After a four-parameter ($\Delta\varepsilon_1$, $\varepsilon_{\infty 1}$, $\Delta\varepsilon_2$, $\varepsilon_{\infty 2}$) curve fitting, as Fig. 10 illustrates, better modeling of the phase and the attenuation factor can be achieved. Also, the Huray modeled surface

roughness correction factor has a better match with the initially extraction results. Comparison of both single mode extractions attempts (using one-term and two-term Djordjevic models) with the "duo-mode" extraction results is illustrated in Fig.11, demonstrating a good match for the tan δ extracted using the two-term Djordjevic model.

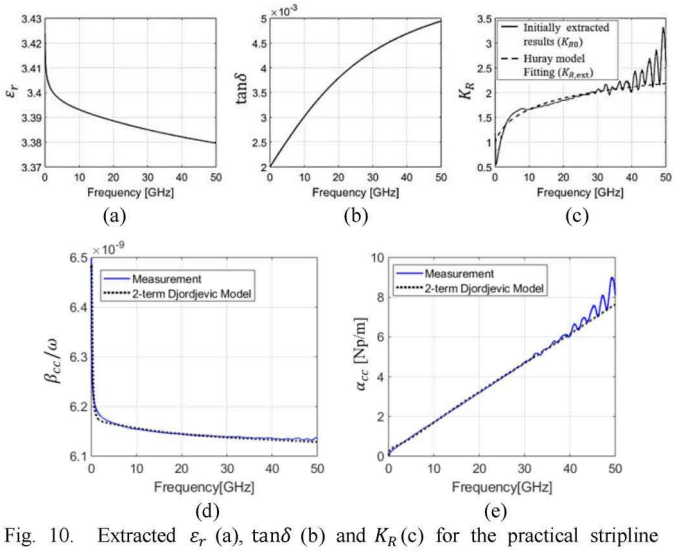

Fig. 10. Extracted ε_r (a), tanδ (b) and K_R (c) for the practical stripline assuming the two-term Djordjevic model. The modeled phase (d) and attenuation factor (e) are compared with the measurement results.

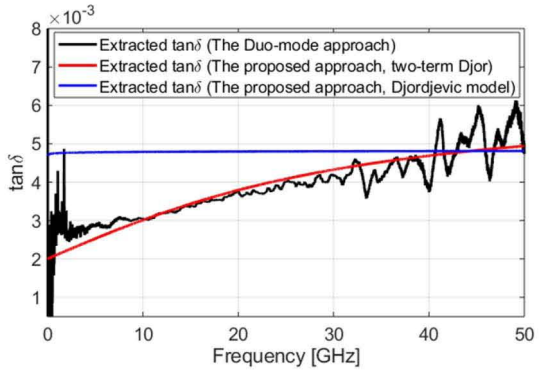

Fig. 11. Dielectric loss extracted with the proposed methodology in comparison with the "duo-mode" method.

V. Conclusion

A new PCB material properties extraction method is proposed in this paper. After conducting the sensitivity analysis, we demonstrate that surface roughness has negligible impact to phase constant (β) and the frequency-dependence of $\beta$is mainly determined by ε_r. Since the frequency-dependence of ε_r is also related to the dielectric dissipation factor (tanδ) due to causality, β is used for tanδ extraction. Compared to the traditional "Root-Omega" approach, the proposed method potentially might achieve better accuracy.

References

[1] M. Y. Koledintseva, T. Vincent, A. C. Scogna, S. Hinaga, "Method of Effective Roughness Dielectric in a PCB: Measurement and Full-Wave Simulation Verification", *IEEE Trans. Electromagn. Compat.*, vol.57, no.4, Aug. 2015. pp.807-814

[2] A. Koul, M. Y. Koledintseva, S. Hinaga, J. L. Drewniak, "Differential extrapolation method for separating dielectric and rough conductor losses in printed circuit boards", *IEEE Trans. Electromagn. Compat.*, vol. 54, no. 2, pp. 421–433, Apr. 2012.

[3] S. Jin, B. Chen, X. Fang, H. Gao, and J. Fan, "Improved 'root-omega' method for transmission-line based material property extraction for multi-layer PCBs", *IEEE Trans. Electromagn. Compat.*, vol. 59, no. 4, pp. 1356–1367, Mar. 2017.

[4] S. Jin, X. Fang, B. Chen, H. Gao, X. Ye, J. Fan, "Validating the transmission-line based material property extraction procedure including surface roughness for multilayer PCBs using simulations", in *Proc. IEEE Int. Symp. EMC*, Ottawa, CN, USA, Jul. 25–29, 2016, pp. 472–477.

[5] S. Yong, Y. Liu, H. Gao, B. Chen, S. De, S. Hinaga, D. Yanagawa, J. Drewniak, V. Khilkevich, "Dielectric Dissipation Factor (DF) Extraction Based on Differential Measurements and 2-D Cross-sectional Analysis", in *Proc. IEEE Int. Symp. EMC*, Long Beach, CA, USA, 30 Jul-3, 2018, pp. 217-222.

[6] S. Yong, V. Khilkevich, Y. Liu, H. Gao, S. Hinaga, S. De, D. Padilla, D. Yanagawa, J. Drewniak, "Dielectric Loss Tangent Extraction Using Modal Measurements and 2-D Cross-sectional Analysis for Multilayer PCB", *IEEE Trans. Electromagn. Compat.*, Early Access

[7] Y. Chen, H. Deng, B. Chen, R. Zai, J. Hsu, X. Ye, J. Fan, J. Drewniak, "Signal-signal D-probe and unified launch pad designs", *IEEE Electromagnetic Compatibility Magazine*, vol. 7, no. 3, 3rd quarter 2018. pp. 101-106.

[8] D. M. Pozar, "Microwave Engineering". Fourth Edition, John Wiley & Sons, Inc, 2012

[9] C. R. Paul, "Analysis of Multiconductor Transmission Lines", 2nd Edition, John Wiley & Sons, Inc, 2008.

[10] E. Bracken, "A Causal Huray Model for Surface Roughness", *DesignCon 2012*

[11] V. D-Zdorov, B. Simonovich, I. Kochikov, "A Causal Conductor Roughness Model and its Effect on Transmission Line Characteristics", *DesignCon 2018*

[12] S. Hall, H. Heck, "Advanced signal integrity for high speed digital designs," John Willey & Sons Inc., Hoboken, NJ, 2009.

[13] X. Sun, Y. Guo, Y. Sun, K. Song, L. Ye, X. Ye, J. L. Drewniak, J. Fan, "Causality Analyzing for Transmission Line with Surface Roughness", in *Proc. Int. Symp. IEEE Electromagn.Compat.*, New Orleans, LA, 2019, pp. 516-521.

[14] A. R. Djordjevic, R. M. Biljic, V. D. Likar-Smiljanic and T. K. Sarkar, "Wideband frequency-domain characterization of FR-4 and time-domain causality", IEEE *Trans. on Electromag. Compat*, Nov. 2001, pp. 662-667.

[15] S. Hall, S. G. Pytel, P. G. Huray, D. Hua, A. Moonshiram, G. A. Brist, and E. Sijercic "Multigigahertz Causal Transmission Line Modeling Methodology Using a 3-D Hemispherical Surface Roughness Approach", *IEEE Trans. Microw. Theory Tech.*, vol. 55, no. 12, Dec. 2007, pp. 2614 – 2624

[16] ANSYS, Inc., ANSYS Electronics Desktop Online Help – 2D Extractor (2018 release), Canonsburg, PA, USA, 2018

[17] Coleman, T.F. and Y. Li. "An Interior, Trust Region Approach for Nonlinear Minimization Subject to Bounds." SIAM Journal on Optimization, Vol. 6, 1996, pp. 418–445

[18] Q. Huang, J. Li, J. Zhou, W. Wu, Y. Qi, and J. Fan, "De-embedding method to accurately measure high-frequency impedance of an O-shape spring contact", in *Proc. Int. Symp. IEEE Electromagn.Compat.*, 2014, pp. 600–603.

[19] B. Chen, J. He, Y. Guo, S. Pan, X. Ye, J. Fan, "Multi-Ports (2^n) 2×-Thru De-Embedding: Theory, Validation, and Mode Conversion Characterization", *IEEE Trans. Electromagn. Compat.*, vol. 61, no. 4, Aug 2019.

[20] S. Yong, Y. Liu, H. Gao, S. Hinaga, S. De, D. Padilla, D. Yanagawa, J. Drewniak, V. Khilkevich, "A Practical De-embedding Error Analysis Method Based on Statistical Circuit Models of Fixtures," in *Proc. Int. Symp. IEEE Electromagn.Compat.*, New Orleans, LA, USA., pp. 45-50.